SUPPORTING INFORMATION

Fine-tuning the bio-nano interface of superfluorinated nanoprobes enhances cell labeling for ^{19}F-MR imaging

Lodovico Gatti[1,2,a,†], Cristina Chirizzi[1,†], Giulia Rotta[3,b], Pietro Milesi[1], María Sancho-Albero[4,5,6,c], Victor Sebastián[4,5,6], Anna Mondino[3], Jesús Santamaría[4,5,6], Pierangelo Metrangolo[1], Linda Chaabane[2,d,*] and Francesca Baldelli Bombelli[1,*]

[1] Department of Chemistry, Materials and Chemical Engineering "Giulio Natta", Politecnico di Milano, Milano 20131, Italy
[2] Institute of Experimental Neurology (INSpe) and Experimental Imaging Center (CIS), IRCCS San Raffaele Scientific Institute, Milano, 20132, Italy
[3] Lymphocyte Activation Unit, Division of Immunology, Transplantation and Infectious Diseases, IRCCS San Raffaele Scientific Institute, Via Olgettina, 58, 20132, Milan, Italy
[4]Instituto de Nanociencia y Materiales de Aragón (INMA), CSIC-Universidad de Zaragoza, Zaragoza, Spain.
[5] Department of Chemical Engineering and Environmental Technologies, University of Zaragoza, Zaragoza, Spain.
[6] Networking Research Center on Bioengineering Biomaterials and Nanomedicine (CIBER-BBN), Madrid, Spain.

Present address:
[a] Department of Experimental Oncology, IEO, European Institute of Oncology IRCCS, via Adamello 16, Milano, 20139, Italy
[b] Philochem AG, Libernstrasse 3, Otelfingen, 8112, Switzerland
[c] Department of Biochemistry and Molecular Pharmacology, Istituto di Ricerche Farmacologiche Mario Negri IRCCS, Via Mario Negri 2, Milano, 20156, Italy
[d] Euro-BioImaging ERIC, Institute of Biostructures and Bioimaging (IBB), Italian National Research Council (CNR), Via Nizza 52, Torino, 10126, Italy

†These authors have equally contributed

***Corresponding authors:**

Francesca Baldelli Bombelli, Department of Chemistry, Materials and Chemical Engineering "Giulio Natta", Politecnico di Milano, Milano 20131, Italy. E-mail: francesca.baldelli@polimi.it

Linda Chaabane, Euro-BioImaging ERIC, Institute of Biostructures and Bioimaging (IBB), Italian National Research Council (CNR), Via Nizza 52, Torino, 10126, Italy. E-mail: linda.chaabane@cnr.it

Contents

Figures

Tables

1. Procedure to formulate PERFECTA@PLGA nanoparticles (^{19}F-PLGA NPs)

1.1 ^{19}F-PLGA-NaC and ^{19}F-PLGA-PVA: PERFECTA (20 mg) is firstly dissolved in the organic solvent (1.5 mL of EtOAc) and heated up to 65^{o} C. It is then added to a solution of the same organic phase containing PLGA (20 mg). 24 mg of Sodium Cholate (NaC) or 100 mg of Polyvinyl alcohol (PVA) are dissolved in 4 or 5 mL of aqueous solution, respectively. After the complete dissolution of the surfactant, the mixture of the organic solution containing both PERFECTA and PLGA is rapidly mixed by pipetting it up and down and dropwise added to the aqueous solution. The two solutions are then sonicated through a tip sonication at 60W for 25 seconds. The obtained solution is stirred magnetically for 3h at room temperature and then the excess of the organic phase is removed by rotary evaporation setting an initial pressure of 250 mbar and lowering by 10 mbar step until 70 mbar pressure at which it remains for 20 minutes. The suspension is finally washed in milliQ water (mQw) through centrifugation at 10733*g* for 40 minutes (4^{o} C), collected and re-suspended in 1 ml of mQw.

1.2 ^{19}F-PLGA-PVA-CS: PERFECTA (30 mg) is firstly dissolved in the organic solvent (1.5 mL of EtOAc) and heated up to 65^{o} C. It is then added to a solution of the same organic phase containing PLGA (20 mg). In order to prepare a stable aqueous solution, 24mg of chitosan are dissolved in 5mL of mQw containing acetic acid 1% (V/V) and the solution is stirred overnight at room temperature. After complete dissolution, CS solution is filtered by 0.2 μm pore size filter. 100 mg of PVA are then dissolved in the aqueous phase previously described. The mixture of the organic solution containing both PERFECTA and PLGA is rapidly mixed by pipetting it up and down and dropwise added to the aqueous solution. The two solutions are then sonicated through a tip sonication at 60W for 25 seconds. The obtained phase is stirred magnetically for 3h at room temperature and then the excess of the organic phase is removed by rotary evaporation setting an initial pressure of 250 mbar and lowering by 10 mbar step until 70 mbar pressure at which it remains for 20 minutes. The suspension is finally washed in mQw through centrifugation at 10733*g* for 14 minutes (4^{o} C), collected and re-suspended in 1 ml of mQw.

1.3 ^{19}F-PLGA-PVA-CS NPs development and optimization

For this purpose, in addition to the well-established ^{19}F-PLGA-NaC and ^{19}F-PLGA-PVA stabilized NPs,[1] a new formulation was developed. In fact, considering the enhanced

bioavailability, higher specificity and sensitivity related to the chitosan-coated (CS-coated) polymeric nanosystems, an improvement in cell internalization of the optimized CS-coated ^{19}F-PLGA NPs was expected.

In detail, the CS amount was initially maintained constant (0.2 wt/wt CS/PLGA) and the desired NP size suitable for *in vitro* applications (< 250 nm), was ensured using PVA contents ≥ 1% w/V (Supplementary information Figure S1 A and S1 B).However, while this set-up allowed to reach a promising PERFECTA loading which was comparable to the control (ctrl) uncoated condition (39 - 41% vs 34%, for CS and ctrl respectively; Figure S1 C), a higher chitosan quantity was clearly needed to get a more positive superficial charge (Figure S1 D). With this in mind, a larger range of CS concentrations was investigated (0 - 1 wt/wt CS/PLGA) and results showed as an amount = 0.8 wt/wt CS/PLGA was essential to reach optimal colloidal properties (D_H = 218 ± 2 nm and PDI < 0.25) together with an increased positive superficial charge = 19±8 mV (Figure S1 E and S1 F).

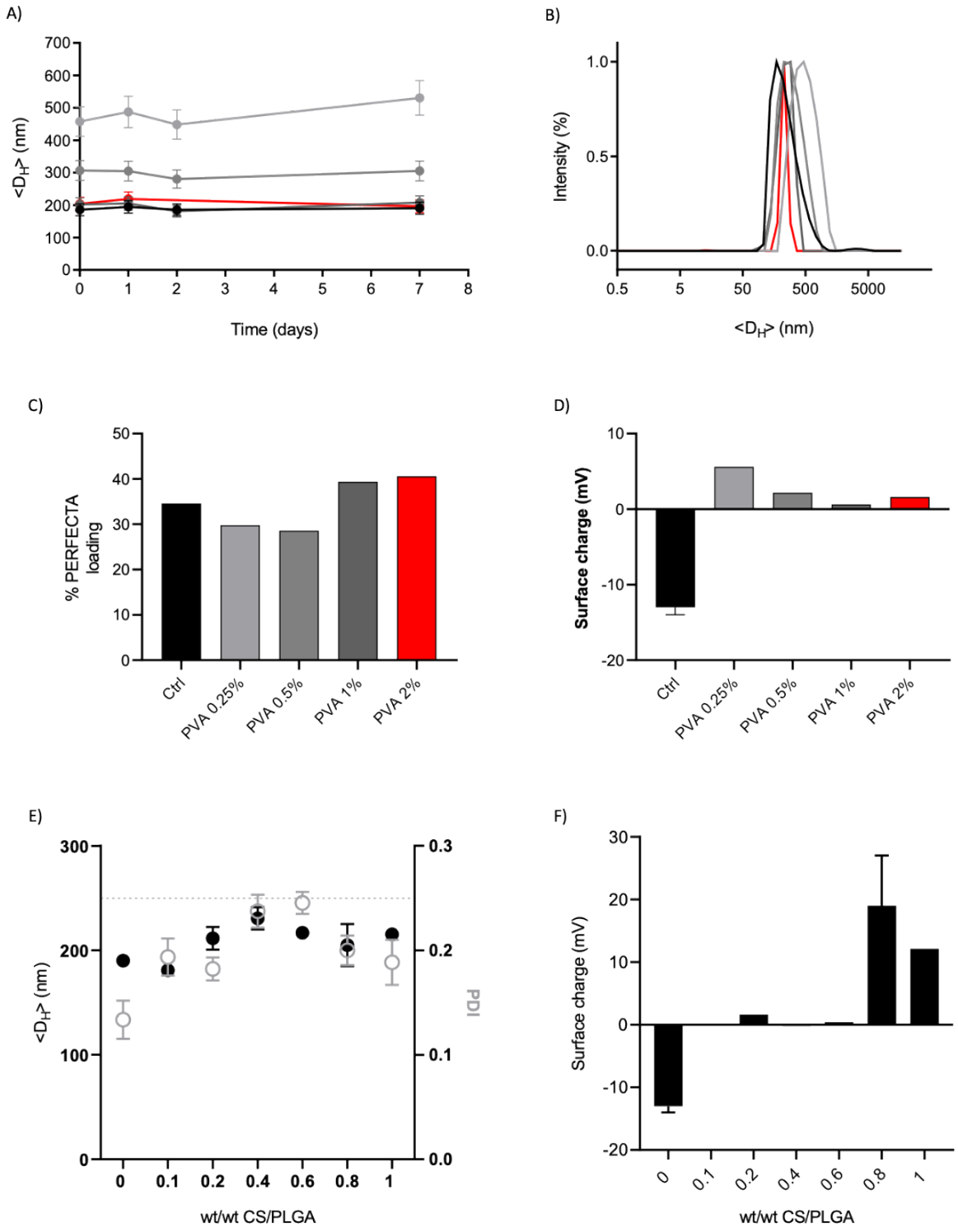

Figure S1: Optimization of chitosan coated ^{19}F-PLGA NPs. Impact of the PVA content on the CS coating efficiency and relation between the chitosan coating entity and NPs surface charge. A) Plot of the zeta-averaged hydrodynamic diameters versus time and B) Intensity-weighted size distribution related to different PVA concentrations (0,25%; 0.5%; 1%; and 2% w/V). C) Evaluation of PERFECTA loading and D) NPs surface charge as a function of the PVA content. E) Plot of the Zeta-averaged hydrodynamic diameters (left Y

axis, black), corresponding PDIs over time (right Y axis, grey) and F) evaluation of the surface charge of ^{19}F-PLGA NPs formulated with a constant PVA content (2% w/V) and a wide range of chitosan concentrations (0 - 1 wt/wt CS/PLGA).

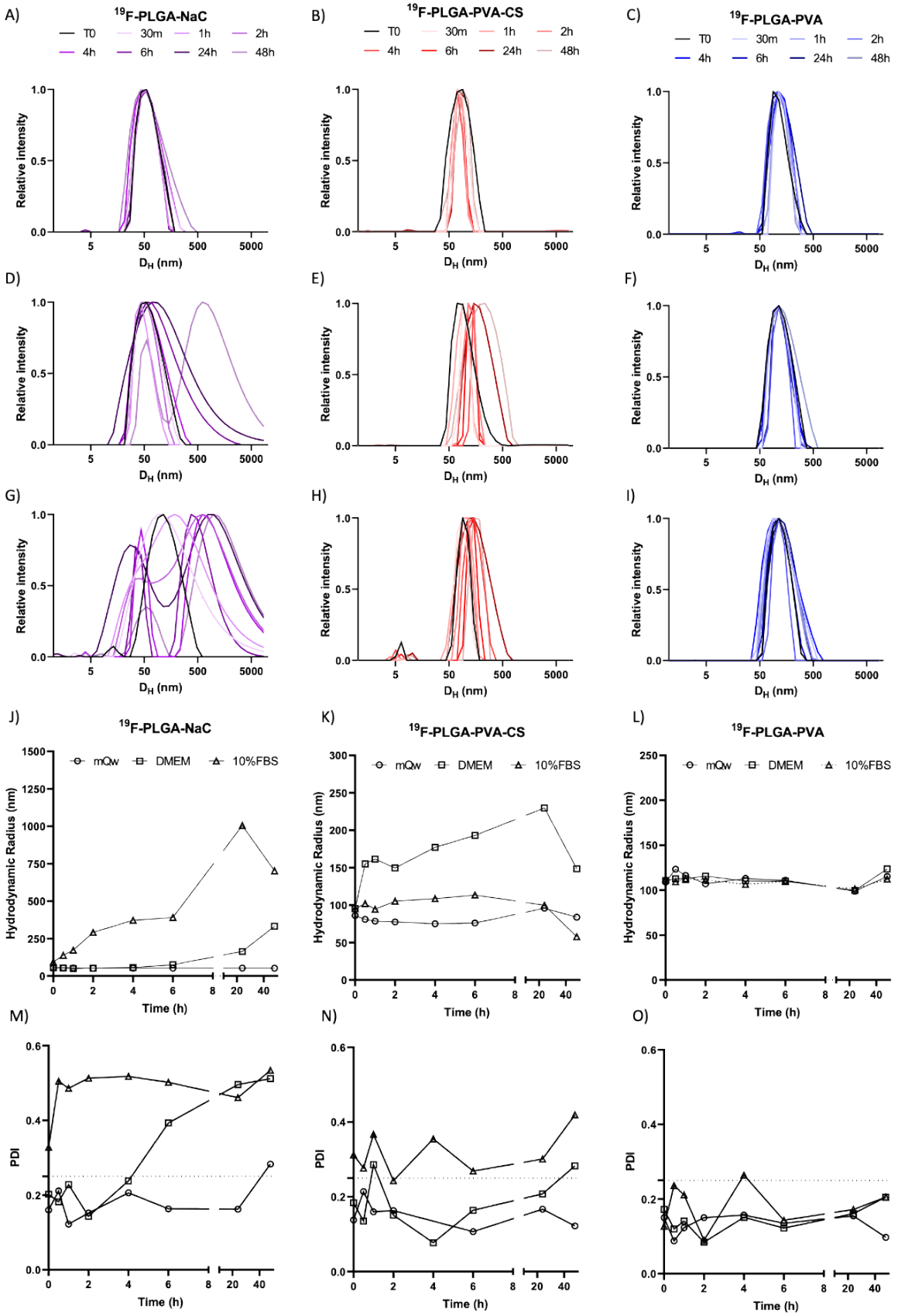
A)
^{19}F-PLGA-NaC
T0
30m
1h
2h
4h
6h
24h
48h
Relative intensity
D_H (nm)
B)
^{19}F-PLGA-PVA-CS
C)
^{19}F-PLGA-PVA
D)
E)
F)
G)
H)
I)
J)
^{19}F-PLGA-NaC
mQw
DMEM
10%FBS
Hydrodynamic Radius (nm)
Time (h)
K)
^{19}F-PLGA-PVA-CS
L)
^{19}F-PLGA-PVA
M)
PDI
N)
O)

Figure S2: Effects of culture medium and protein on ^{19}F-PLGA NPs. The stability properties of ^{19}F-PLGA-NaC NPs are not maintained in all proposed media. Indeed, its stability in mQw (A) is totally lost in DMEM after 48h (D) and in DMEM + 10%FBS (G) just after 2h. This behaviour is also confirmed by both hydrodynamic radius (J) and PDI (M) plots as a consequence of the protein adsorption on the NPs surface. ^{19}F-PLGA-PVA-CS shows stable colloidal properties in mQw (B) and DMEM (E) up to 48h as confirmed by hydrodynamic radius (K) and PDI (N) plots, while, for the DMEM + 10%FBS (H) conditions the stability is not totally maintained and the size increases during the first 24 hours due to the assimilation of FBS proteins. ^{19}F-PLGA-PVA is perfectly stable in mQw (C), DMEM (F) and DMEM + 10%FBS (I). In all these media the formulation maintains its colloidal stability as showed by the constant hydrodynamic radius (L) and PDI (O).

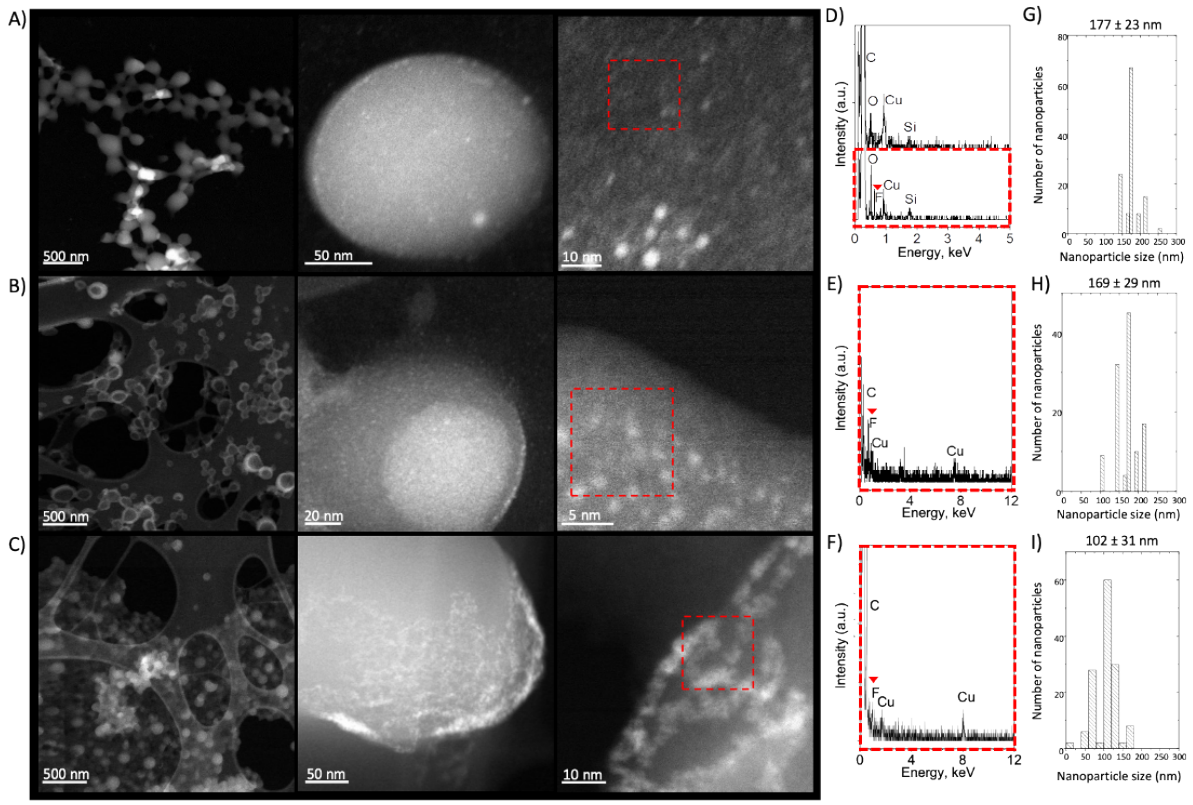

Figure S3: HAADF-STEM images of ^{19}F-PLGA-NaC (A), ^{19}F-PLGA-PVA-CS (B) or ^{19}F-PLGA-PVA (C) nanoparticles at different magnification. The EDS spectrum showed the chemical composition of control (D: empty NPs, top of the figure) compared to ^{19}F-PLGA NPs (red boxes: D, E and F for NaC, PVA-CS and PVA stabilized NPs, respectively). Desiccated particle size distributions were generated by measuring particle diameters in the TEM images for each ^{19}F-PLGA NPs (G: NaC, H: CS-PVA, and I: PVA). Reproduced with permission from ref (1). Copyright 2022 Elsevier B.V.

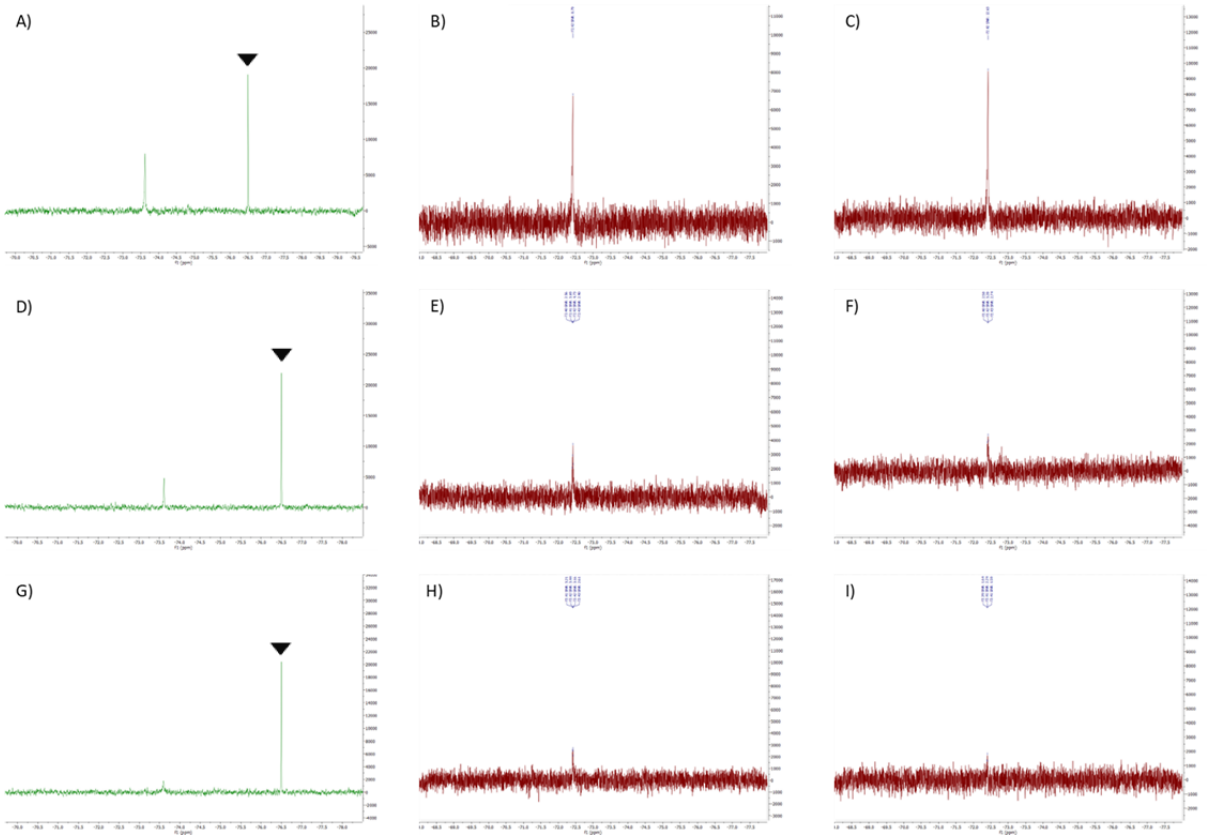

Figure S4: Efficiency of labeling overtime. ^{19}F-NMR analyses of the supernatants collected from different samples of labeled cells after 24 (A, B, C), 48 (D, E, F) and 72 hours (G, H, I) post labeling with ^{19}F-PLGA NaC. Quantification of fluorine content is reported for one sample/condition (A: 24h, D: 48h, G: 72h). For this purpose, a TFA reference (δ: -75ppm, black arrow) containing 0.48-1×10^{16} ^{19}F atoms was used. Results showed a residual fluorine signal of 1.45 (A) or 0.4 ×10^{17} fluorine atoms (D and G), corresponding to ≤ 1% of the total uptaken amount.

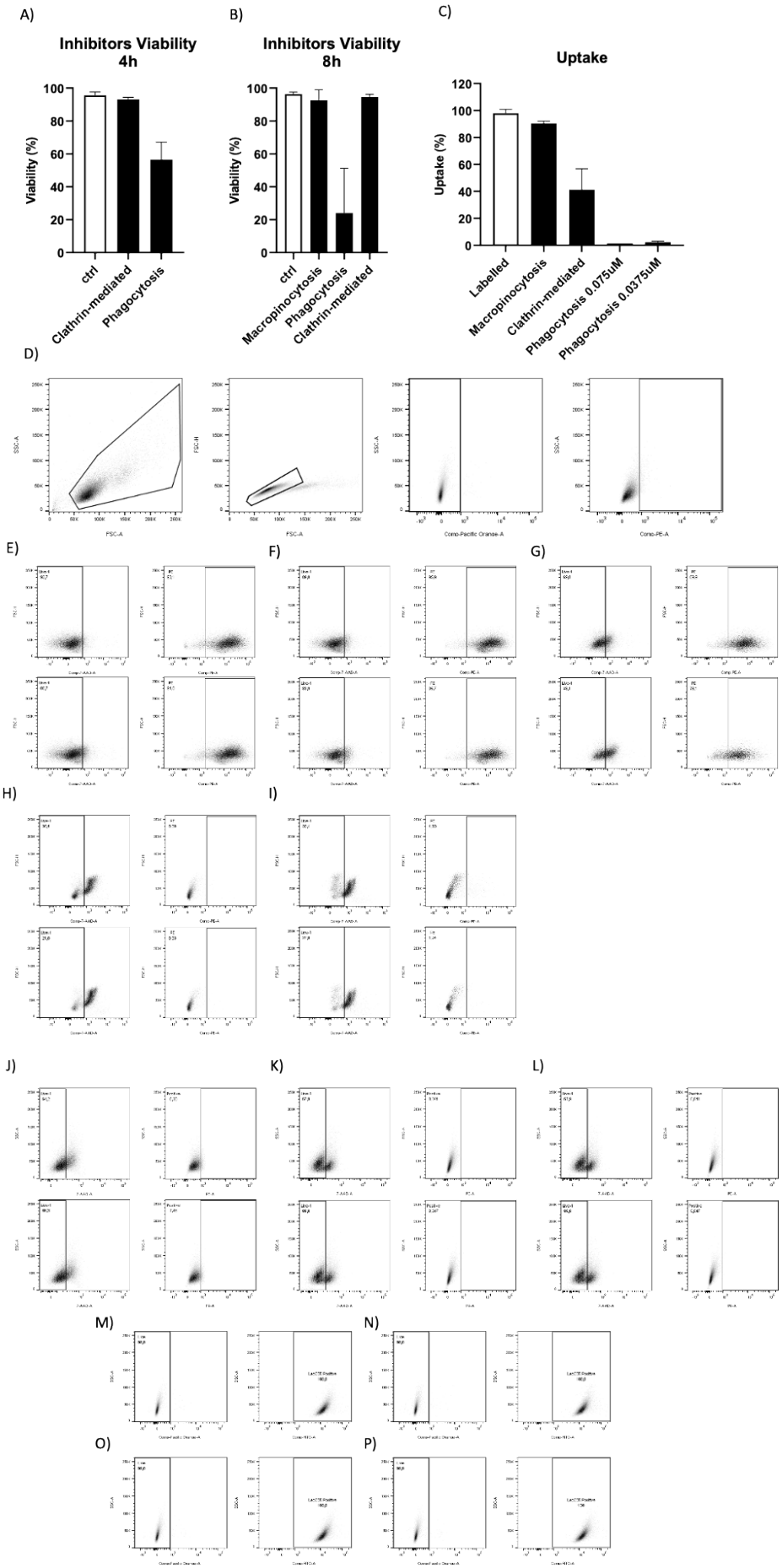
A)
Inhibitors Viability 4h
Viability (%)
ctrl
Clathrin-mediated
Phagocytosis
B)
Inhibitors Viability 8h
Viability (%)
ctrl
Macropinocytosis
Phagocytosis
Clathrin-mediated
C)
Uptake
Uptake (%)
Labelled
Macropinocytosis
Clathrin-mediated
Phagocytosis 0.075uM
Phagocytosis 0.0375uM
D)
E)
F)
G)
H)
I)
J)
K)
L)
M)
N)
O)
P)

Figure S5: Gating strategy and inhibition of preferential substrate for uptake pathway. Viability of BV2 cells in presence of inhibitors for phagocytosis and clathrin-mediated endocytosis after 4h (A) and 8h (B) including also macropinocytosis inhibitors. C) First test of preferential uptake pathways for BV2 related to ^{19}F-PLGA-PVA-CS NPs in presence (4h) of inhibitors for macropinocytosis (400 μM), clathrin-mediated (7 μM) and two different concentrations of phagocytosis inhibitor (0.075 and 0.0375 μM). This last assay was performed to select the optimal dose of inhibitor for BV2 cells compared to literature. [2–5] D) Gating strategy. Cells were gated on the linear side scatter area (SSC-A) versus the forward-angle light scatter area (FSC-A) to exclude the debris. Secondly, forward scatter height (FSC-H) versus forward scatter area (FSC-A) density plot was used to exclude doublets. Successively, live cells were selected using the 7AAD stain. Labelling efficiency (comp: PE-A, indicative for RhodamineB) was evaluated considering the fluorescence signal. E-I) Live (comp: 7-AAD-A) and RhodamineB (comp: PE-A) panels of fluorescence used to understand if cells in panel C were successfully labelled and still viable. J, K, L) Second test performed on Phenylarsine Oxide (PAO, phagocytosis inhibitor) at a lower concentration due to high toxicity observed at higher doses. The concentration equal to 0.0075 μM (M) was chosen as more suitable in terms of viability and inhibition. M-P) Test performed on Filipin III (inhibitor for caveolin-mediated endocytosis) at different doses.

A)

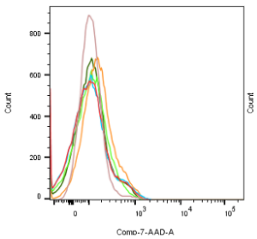

B)

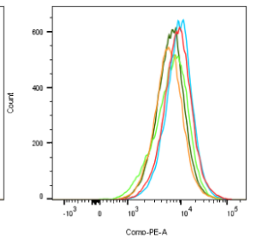

Sample Name	Sample Name	Mean : Comp-PE-A
Samples_Unlabelled.fcs		
Samples_Labelled s2.fcs	*Samples_Labelled s2.fcs*	*10690*
Samples_Amiloride s3.fcs	Samples_Amiloride s3.fcs	10969
Samples_CPZ S7.fcs	Samples_CPZ S7.fcs	7195
Samples_PAO s8.fcs	Samples_PAO s8.fcs	8212
Samples_Filipin s9.fcs	Samples_Filipin s9.fcs	7643

C)

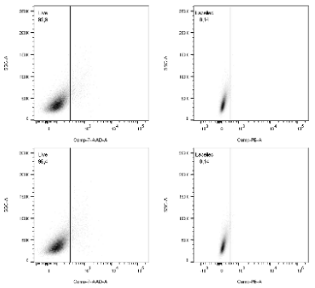

D)

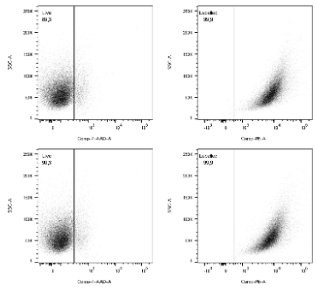

E)

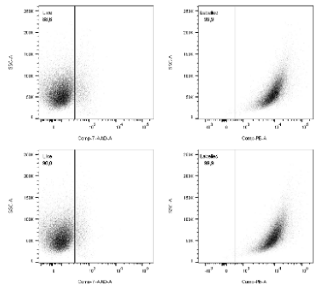

F)

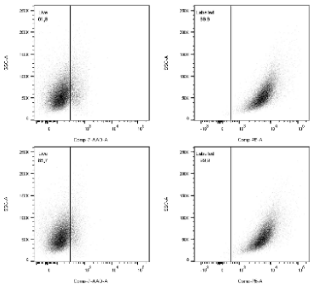

G)

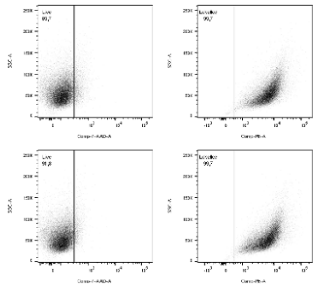

H)

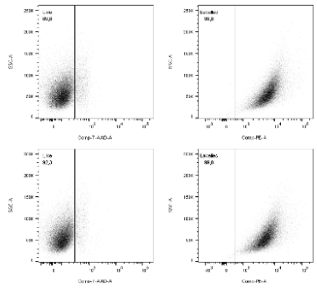

I)

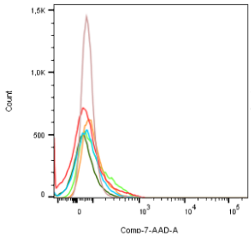

J)

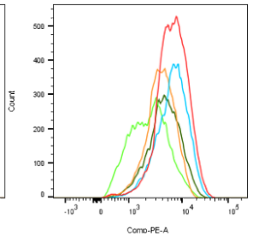

Sample Name	Sample Name	Mean : Comp-PE-A
Samples_Unlabelled s1.fcs		
Samples_Labelled s2.fcs	*Samples_Labelled s2.fcs*	*7910*
Samples_Amiloride s3.fcs	Samples_Amiloride s3.fcs	7682
Samples_CPZ s7.fcs	Samples_CPZ s7.fcs	4454
Samples_PAO s8.fcs	Samples_PAO s8.fcs	3124
Samples_Filipin s9.fcs	Samples_Filipin s9.fcs	5514

K)

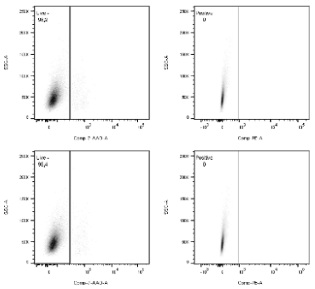

L)

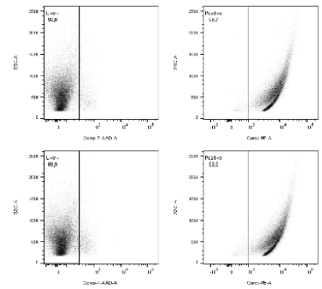

M)

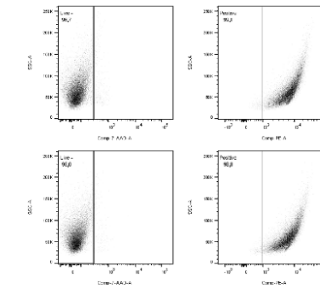

N)

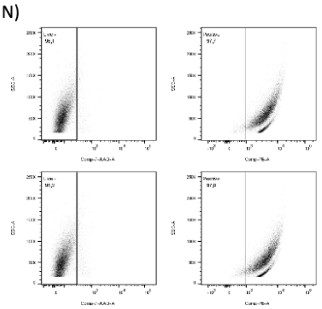

O)

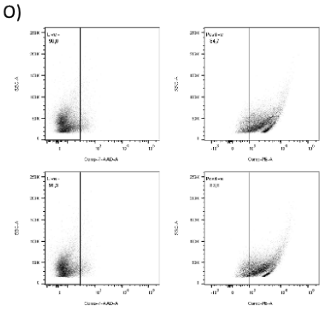

P)

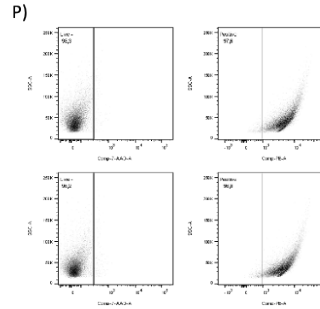

Figure S6: Raw data of ^{19}F-PLGA-PVA-CS and ^{19}F-PLGA-NaC uptake inhibition on BV2. A-B) Flow cytometry histograms of live (A, comp: 7-AAD-A) and RhodamineB (B, comp: PE-A) positive cells on BV2 cells labelled with ^{19}F-PLGA-PVA-CS. B) Histogram of inhibited condition in comparison to labeled control for ^{19}F-PLGA-PVA-CS NPs. C-H) Flow Cytometry gating on live and RhodamineB positive channel for each sample incubated with ^{19}F-PLGA-PVA-CS. C) Unlabelled control used to determine the fluorescent threshold and thus select NPs-loaded cells. Endocytic pathway inhibition using amiloride hydrochloride for macropinocytosis (D), phenylarsine oxide for phagocytosis (E), chlorpromazine for clathrin-mediated (G), labeled control used to define the upper threshold for non-inhibited condition (F), and for caveolin-mediated (H). I-J) Flow cytometry histograms of live (I, comp: 7-AAD-A) and RhodamineB (J, comp: PE-A) positive cells on BV2 cells labelled with ^{19}F-PLGA-NaC. K-P) Gating on live and RhodamineB positive channel for each sample incubated with ^{19}F-PLGA-NaC. K) Unlabelled control used to determine the fluorescence threshold and thus select NPs-loaded cells. Endocytic pathway inhibition using amiloride hydrochloride for macropinocytosis (L), phenylarsine oxide for phagocytosis (M), labeled control used to define the upper threshold for non-inhibited condition (N), chlorpromazine for clathrin-mediated (O) and filipin III for caveolin-mediated (P).

Table S1: T_1 and T_2 measurements of the three ^{19}F-PLGA NPs acquired by ^{19}F-MRI.

Sample	T_1 (ms)	T_2 (ms)
^{19}F-PLGA-NaC [1]	**260 ± 41**	**198 ± 17**
^{19}F-PLGA-PVA-CS	**340 ± 65**	**204 ± 32**
^{19}F-PLGA-PVA [1]	**355 ± 59**	**220 ± 29**

Table S2: Description of the experimental details used for cellular uptake inhibition**.**

Pharmacological inhibitors	Concentration range (µM)	Endocytic pathway involved
Phenylarsine oxide	**0.0075-1.2**	**Phagocytosis**
Amiloride chloride	**25-400**	**Macropinocytosis**
Filipin III	**1.9 -30**	**Caveolin-mediated**
Chlorpromazine chloride	**2-56**	**Clathrin-mediated**

3. Bibliography:

1. Chirizzi C, Gatti L, Sancho-albero M, et al. Colloids and Surfaces B : Biointerfaces Optimization of superfluorinated PLGA nanoparticles for enhanced cell labelling and detection by 19 F-MRI. *Colloids Surfaces B Biointerfaces*. 2022;220(July):112932. doi:10.1016/j.colsurfb.2022.112932
2. Torres-Vanegas JD, Cruz JC, Reyes LH. Delivery systems for nucleic acids and proteins: Barriers, cell capture pathways and nanocarriers. *Pharmaceutics*. 2021;13(3):1-38. doi:10.3390/pharmaceutics13030428
3. Day R, Estabrook D, Wu C, Chapman J, Togle A, Sletten E. Systematic study of perfluorocarbon nanoemulsions stabilized by polymer amphiphiles. Published online 2020.
4. Fitzner D, Schnaars M, Van Rossum D, et al. Selective transfer of exosomes from oligodendrocytes to microglia by macropinocytosis. *J Cell Sci*. 2011;124(3):447-458. doi:10.1242/jcs.074088
5. Hsiao IL, Hsieh YK, Chuang CY, Wang CF, Huang YJ. Effects of silver nanoparticles on the interactions of neuron- and glia-like cells: Toxicity, uptake mechanisms, and lysosomal tracking. *Environ Toxicol*. 2017;32(6):1742-1753. doi:10.1002/tox.22397